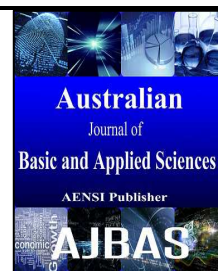




AUSTRALIAN JOURNAL OF BASIC AND APPLIED SCIENCES

ISSN:1991-8178 EISSN: 2309-8414
Journal home page: www.ajbasweb.com



Sensing Properties of (In₂O₃:Eu) Thin Films

¹Bushra A. Hasan, ²Jamal. M. Rzaij and ²Iftikhar. M. Ali

¹University of Baghdad, College of Science, Department of Physics

²University of Anbar, College of Science, Department of Physics

Address For Correspondence:

Bushra A.Hasan, University of Baghdad, College of Science, Department of Physics.
E-mail: bushra_abhasan@yahoo.com

ARTICLE INFO

Article history:

Received 12 February 2016

Accepted 18 March 2016

Available online 20 April 2016

Keywords:

ABSTRACT

Thin films of iridium doped indium oxide (In₂O₃:Eu) with different doping ratio (0, 3, 5, 7, and 9%) are prepared on glass and single crystal silicon wafer substrates using spray pyrolysis method. The goal of this research is to investigate the effect of doping ratio on the structural, optical and sensing properties. The structure of the prepared thin films was characterized at room temperature using X-ray diffraction. The results showed that all the undoped and doped (In₂O₃:Eu) samples are polycrystalline in structure and nearly stoichiometric. UV-visible spectrophotometer in the wavelength range (200-1100nm) was used to determine the optical energy gap and optical constants. The optical transmittance of 83% and the optical band gap of 5.2eV for pure In₂O₃ declare drastic reduction as Eu dopant introduce to the indium oxide and then return to increase with further increase of doping ratio. The best figure of merit of the films was achieved for pure sample.

INTRODUCTION

Non-stoichiometric transparent conducting oxides (TCO) such as tin oxide, cadmium oxide, zinc oxide, indium oxide, etc., find a wide variety of applications in microelectronic and optoelectronic devices because of their high optical transmittance in the visible range with high electrical conductivity. Among these, indium oxide In₂O₃ is an n-type degenerate semiconducting oxide which is finds optoelectronic applications such as flat panel displays, solar cells, photodiodes (Fortunato, E., 2007, Biyikli, N., 2001). In₂O₃ is a wide-bandgap (3.75 eV) n-type semiconductor, with appreciable single-crystal mobility (160 cm² V⁻¹ s⁻¹) and high film transparency in the visible region (> 90%) (Vygranenko, Y., 2007). For the past three decades many researchers have reported on the physical properties of In₂O₃ films formed by different deposition methods such as flash evaporation (Kaleemulla, S., 2007), electron beam evaporation (Subrahmanyam, A., U.K. Barik, 2005), dc/rf magnetron sputtering (Radhakrishna, B., 2000, Chen, L.C., S.C. Liu, 2006), laser deposition, molecular beam epitaxy (Huang, M.H., 2001), chemical vapor deposition (Bourlang, A., 2008, Prathap, 2006), sol-gel process (Sailer, R.A., 2008), spray pyrolysis (Flores, M.A., 2008; Moholkar, A.V., 2008), electrochemical deposition (Ghimbeu, C.M., 2008) were employed for preparing indium oxide films to meet present day science and technological requirements. But less work has been reported on the influence of doping with Eu which affects the hole properties of In₂O₃ films prepared by spray pyrolysis method. The aim of this research is to determine the effect of doping ratio the structural, optical, and electrical properties of In₂O₃ thin films prepared at room temperature.

Basic Considerations:

The fundamental absorption edge of polycrystalline or crystalline semiconductors is the region in which the electrons are excited from the valence band V.B to the conduction band C.B by absorbing the incident photons

Open Access Journal

Published BY AENSI Publication

© 2016 AENSI Publisher All rights reserved

This work is licensed under the Creative Commons Attribution International License (CC BY).

<http://creativecommons.org/licenses/by/4.0/>



Open Access

To Cite This Article: Bushra A.Hasan, Jamal.M.Rzaij and Iftikhar .M.Ali., Sensing Properties of (In₂O₃:Eu) Thin Films. *Aust. J. Basic & Appl. Sci.*, 10(8): 143-150, 2016

these photons should have energy equal or greater than the energy gap of semiconductors. The absorption coefficient (α) which is the decrement ratio of incident radiation relative to unit length in the direction of wave propagation inside the medium is relating with the absorbance (A) through the relation (Klopper, W., 1984):-

$$\alpha = \frac{2.303A}{t} \quad (1)$$

Where (t) is the sample thickness. Many researchers (Ho, W.H., 2008; Tauc, J., 1974) put the empirical equation between the optical energy gap (E_g) and energy of the incident photon which is :-

$$(\alpha h\nu) = A(h\nu - E_g)^r \quad (2)$$

Where A is constant, $h\nu$ is the energy of incident photon which can be calculated using the equation:-

$$h\nu = \frac{1240}{\lambda(nm)} \dots \quad (3)$$

r is the order of the optical transition depending on the nature of electronic transition. The transition is called direct if the extremities of V.B and C.B lie at the same K-space, while the transition is called indirect if the transition possible only with phonon assisted ($\Delta k \neq 0$) (Pankov, J., 1971). Thus the value of (r) may be 1/2, 2, 3/2, and 3 corresponding to the allowed direct, allowed indirect, forbidden direct and forbidden indirect transition respectively. The absorption edge become wide for polycrystalline and amorphous semiconductors because of allowed localized states are found in the energy gap, the width of these localized states can be calculated using Urbach Rule (Korotcenkov, G., 2007)

$$\alpha = \alpha_0 e^{h\nu/E_e} \quad (4)$$

Where (α_0) is constant and E_e is the width of localized states.

The optical behavior of materials utilized to determine its optical constants (refractive index (n), extinction coefficient (k), real and imaginary parts of dielectric constants (ϵ_1 , ϵ_2)). Several methods were proposed to determine the optical constants, they involve spectrophotometric measurements of reflectance (R) and transmittance (T) of sample in the wavelength range. The extinction coefficient (imaginary part of the refractive index) can be calculated by the relation (Pankov, J., 1971):

$$k = \frac{\alpha\lambda}{4\pi} \dots (5) \text{ where } \lambda \text{ is the wavelength, } \alpha \text{ is the absorption coefficient which can be obtained using equation (1).}$$

The refractive index (n) can be measured (when the reflectance (R) and (k) are known) by using the equation [22]:

$$n = \sqrt{\frac{4R}{(R-1)^2} - k^2} - \frac{(R+1)}{(R-1)} \quad (6)$$

The complex index (\bar{N}) is given by:

$$\bar{N} = n - ik = \sqrt{\epsilon} \quad (7)$$

Where ϵ is the complex dielectric constant, given by:

$$\epsilon = \epsilon_1 - i\epsilon_2 \quad (8)$$

The parameter ϵ_r is the real part of dielectric constant, ϵ_i is the imaginary part of dielectric constant, from equations (9) and (10) one can obtained :

$$\epsilon_r = n^2 - k^2 \dots \dots \dots (9)$$

$$\epsilon_i = 2nk \dots \dots \dots (10)$$

2. Experiments:

In this work, In_2O_3 thin films were prepared on glass and single crystal silicon wafer P-Type (111) substrates using spray pyrolysis technique. The spray pyrolysis apparatus used in this work consists of a homemade spraying unit, a substrate holder with heater, and an enclosure. The glass substrate is kept on a stainless steel plate. The condition of preparation is listed in table below:

Spray Parameters	Optimum Value/Item
Nozzle-Substrate Distance	30±2 cm
Gas Pressure	1 Bar

Spray Time	5 sec
Stopping Time	10 sec
Substrate Temperature	325 °C
Solution Flow Rate	2 ml/min
Carrier Gas	O ₂
In ₂ O ₃	0.1M
Eu	0.1M
Solvent	HCl

The structural aspects were investigated by X-ray diffraction (PW1840) using Cu $K\alpha$ radiation. Optical transmission for samples was measured with a UV-visible spectrophotometer Cary 100 in the range 200-1100nm.

RESULTS AND DISCUSSION

The XRD pattern of the undoped and Eu-doped In₂O₃ thin film prepared at different doping ratio deposited on glass substrate is shown in Fig. 1. The results show that the as deposited In₂O₃ films was polycrystalline in nature, by increasing the doping ratio the films exhibit a polycrystalline structure with (222) being the dominant orientation. The introduction of iridium to the host prepared films has significant effect on the structure i.e. the crystallinity of the films was worsened, hence the grain size was reduced. The average grain size (particle size) D of the thin films was calculated using the Scherer equation (Korotcenkov, G., 2007): $D = 0.94\lambda/(\beta \cos\theta)$, where λ is the X-ray wavelength, β is the full-width at half-maximum of the (222) diffraction line and θ is the diffraction angle of the XRD spectra. All of the diffraction peaks can be indexed to the cubic In₂O₃ (JCPDS card no. 96-101-0589). No peaks corresponding to Eu are observed, indicating that iridium gets incorporated well into the In₂O₃ lattice. The reduction in the grain size attributed to increase in the density of the grain boundaries. By further increase in the doping ratio, the XRD spectrum tend to approach amorphous structure (Parthibab, S., 2009). The intensity ratio of the peaks (222) orientation decreases along with the doping ratio. By increasing the doping ratio from 0 to 9%, the grain size decreased from 14.5 nm to 8.48 nm and this is in good agreement with the optical data which is found in Table.2. The particle size is found to be 14.5, 14.8, 14.47, 11.5 and 8.48 nm at the doping ratio of 0, 3, 5, 7 and 9% respectively. It can be observed that the crystallite sizes decreases on elevating the doping ratio because the doping decreases the energy of ions or ion clusters prior to collision with the substrates (Jeong, S.H., 2003).

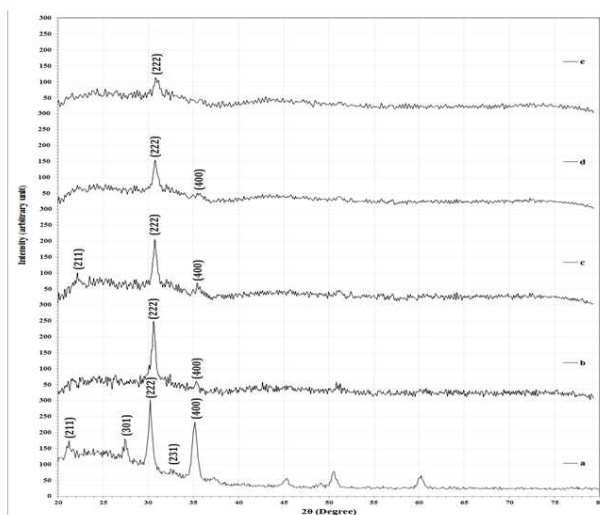


Fig. 1: XRD patterns of In₂O₃:Eu thin films doped with different doping ratio (a) In₂O₃, (b) In₂O₃ doped with 3% Eu, (c) In₂O₃ doped with 5% Eu, (d) In₂O₃ doped with 7% Eu, (e) In₂O₃ doped with 9% Eu.

Table 1: Effect of Eu doping on XRD results of the In₂O₃ thin films.

Sample	2θ (Deg.)	FWHM (Deg.)	d _{hkl} Exp.(Å)	G.S (nm)	d _{hkl} Std.(Å)	hkl	card No.
	21.2000	0.5650	4.1875	14.3048	4.1315	(211)	96-101-0589
	27.4800	0.6120	3.2431	13.3633	3.2002	(301)	96-101-0589
	30.2200	0.5650	2.9550	14.5642	2.9214	(222)	96-101-0589
a	32.8000	0.6350	2.7283	13.0413	2.7047	(231)	96-101-0589
	35.1400	0.5650	2.5518	14.7487	2.5300	(400)	96-101-0589
	37.2400	0.5650	2.4125	14.8373	2.3853	(330)	96-101-0589

	45.2400	0.5880	2.0028	14.6366	1.9847	(341)	96-101-0589
	49.0000	0.6000	1.8575	14.5506	1.8477	(512)	96-101-0589
	50.5600	0.6120	1.8038	14.3557	1.7890	(440)	96-101-0589
	60.1400	0.6350	1.5373	14.4563	1.5256	(622)	96-101-0589
b	30.5900	0.5560	2.9201	14.8130	2.9214	(222)	96-101-0589
	35.3100	0.5400	2.5399	15.4388	2.5300	(400)	96-101-0589
c	22.1000	1.2130	4.0190	6.6730	4.1315	(211)	96-101-0589
	30.7000	0.5690	2.9099	14.4783	2.9214	(222)	96-101-0589
	35.3800	0.4920	2.5350	16.9483	2.5300	(400)	96-101-0589
d	30.7200	0.7150	2.9081	11.5225	2.9214	(222)	96-101-0589
	35.3800	0.6410	2.5350	13.0087	2.5300	(400)	96-101-0589
e	30.7900	0.9710	2.9016	8.4860	2.9214	(222)	96-101-0589

Figure 2 shows the optical transmittance curves as a function of wavelength for the $\text{In}_2\text{O}_3:\text{Eu}$ thin films that are prepared with different doping. It is clear from the figure that the average transmittance of the thin films is more than 85% for wavelengths in the 500–1100 nm range, indicating the good transparency of the thin films. Moreover, it can be seen that the optical transmittance observed in the films decreases with the increase of doping ratio in the first but then increase with continues increase of doping ratio, indeed the transmittance decreases from 85% to 22% with an increase in the doping ratio from 0 to 5% and then return to increase to 32% with further increase of doping ratio. Furthermore, high transmittance in the films may be ascribed to less scattering effects, structural homogeneity and better crystallinity. A red-shift in the absorption edge was observed as iridium added to the host material. Note worthy the red-shift of the cut-off edge take place as a result of reduction in to grain size, arises from doping (Green, L.E., 2003). This may be attributed to the creation of the defect states in the gap or the strain. With the increase of doping ratio from 5 to 9%, there is UV-off shifts to shorter wavelength which is accompanied by increase of band gap as can be seen later, this is known as the Burstein–Moss shift.

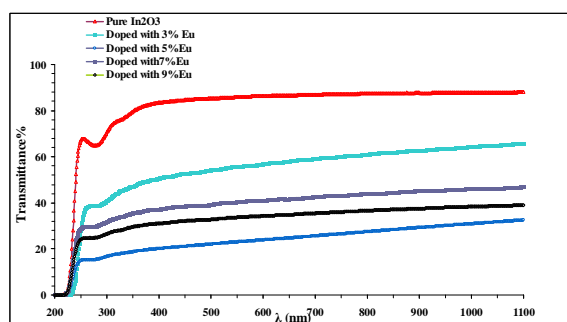


Fig. 2: Transmittance spectra for the Eu-doped In_2O_3 thin films obtained at different doping ratio.

The refractive index (n) of undoped and Eu doped In_2O_3 films with different doping ratio were measured and plotted as function of wavelength (λ) in Fig. 3. It was found that (n) decreased with (λ) in the range (200–1100) nm, on the other hand at $\lambda=500\text{nm}$ which lies in middle of spectrum of the transparent region, the refractive index exhibit to change in non systematic sequence with doping ratio i.e. increases in the first and then decreases with further increase of doping ratio, indeed n increases from (2.08 to 9.01) with increasing of doping ratio from 0 to 5% and then return to decrease when Eu ratio increases to 9%. indicating that the increasing of doping ratio made the samples films more opaque to the incident light in the first but then return be more transparent to the incident light. The dependence of the extinction coefficient (k) on the wavelength is shown in Fig.4. It is evident that the values of (k) were reduced, become smaller at the region beyond the absorption edge, they are relatively small with increasing of (λ). It is remarked that (k) values at $\lambda=500\text{nm}$ increased from (0.082 to 0.284 as Eu introduced to the host material but then k decreases with further increase of Eu. The increasing of k can be attributed to the increasing of absorption coefficient, hence k will be increased according to equation (5), while the decreasing of k is ascribes to eliminating of defect states responsible about the absorption processes in the band gap. Real and imaginary parts of dielectric constant (ϵ_1 and ϵ_2) of undoped and Eu doped In_2O_3 films with different doping ratio were calculated using eqs. (9 and 10). The dependence of (ϵ_r) and (ϵ_i) on (λ) are shown in Figs. (5) and (6), it is concluded that the variation of (ϵ_r) mainly depend on the value of (n^2) because the smaller value of (k) comparison with (n^2), while the imaginary part of dielectric constant (ϵ_i) mainly depend on (k) values which are related to the variation of (α).

The variation of $(\alpha h\nu)^2$ ($\alpha h\nu$)^{1/2} with photon energy ($h\nu$) for direct and indirect allowed transition are plotted in Fig.7 and 8 for undoped and Eu doped In_2O_3 films with different doping ratio, the optical energy gaps are determined which are listed is Table.1. It is clear that direct (E_g) decreases as Eu added to In_2O_3 films, although (E_g) increases with further increase of doping ratio, moreover (E_g) decreases from 5.2 to 3.18 eV

when Eu ratio increase from 0 to 3%nm, while (E_g) increases to 3.5 eV as Eu ratio increases to 9% .Also the indirect energy gap show the same sequence with doping ratio , noteworthy the indirect band gap values are lower than those direct bangap values . The drastic decrease in the energy gap at 3% doping ratio is related that this sample attain maximum particle size (14.8nm) as seen from table.1 .The optical bandgaps obtained for doped films are much lower than that of undoped one. The reduction of the bandgap is in good agreement with the red shift observed from transmittance spectra due to the Burstein–Moss effect .

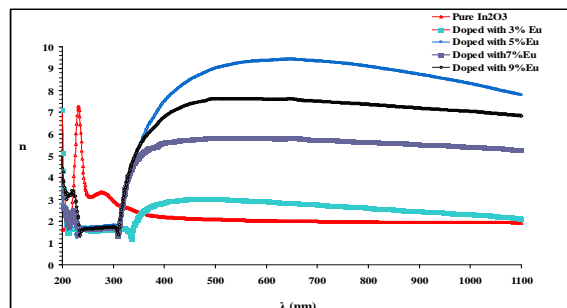


Fig. 3: Variation of refractive index with the wavelength for the Eu-doped In_2O_3 thin films obtained at different doping ratio.

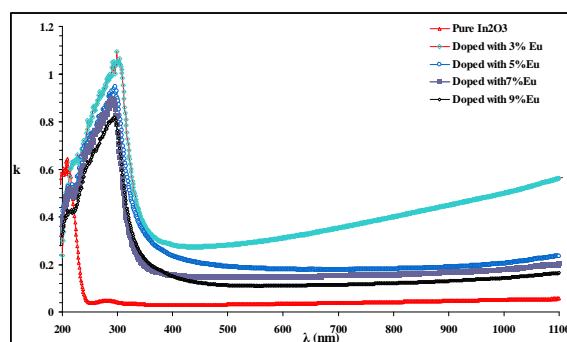


Fig. 4: Variation of extinction coefficient k with wavelength for the Eu-doped In_2O_3 thin films obtained at different doping ratio.

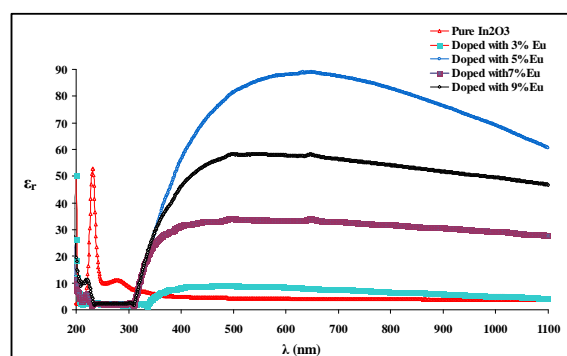


Fig. 5: Variation of ϵ_r with the wavelength for the Eu-doped In_2O_3 thin films obtained at different doping ratio.

The electrical properties were determined. In this work, the gas sensing properties of the In_2O_3 .Eu thin films which are deposited by spray pyrolysis technique was characterized for NO_2 . The sensitivity, (S) of the film is defined as the ratio between the surface resistance of the film in air (R_a) and gas (R_g):
$$S = \frac{(R_{air} \cdot \Omega)}{(R_{gas} \cdot \Omega)}$$

The dynamic response /recovery time cycle for the four samples grown at doping ratio 0,3,5,7,and 9% in NO_2 ambient are shown in Fig. 6. It is obvious that the first sample (undoped sample) has higher sensitivity to the incoming gas and moreover. Generally, it is accepted that a more resistive sample with higher roughness is better compared to another due to its better trapping situation for reducing the gases (Korotcenkov, G., 2004).

Generally, films with higher resistance declared a greater response to the reducing ambient gas. This behavior indicates direct correlation between the gas response and the film stoichiometry. Generally, when the conductivity (resistivity) is low (high), the response to the reducing gases is high. According to XRD results (Fig.1), the undoped sample which shows lower deviation of stoichiometry compared to the residual samples, hence, as expected better sensitivity was observed for the pure sample as shown in Fig.(10).

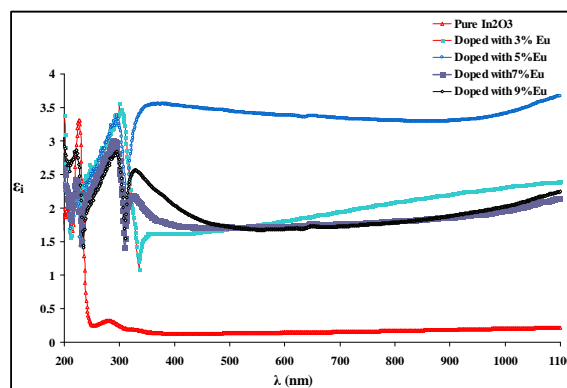


Fig. 6: Variation of ϵ_i with the wavelength for the Eu-doped In_2O_3 thin films obtained at different doping ratio.

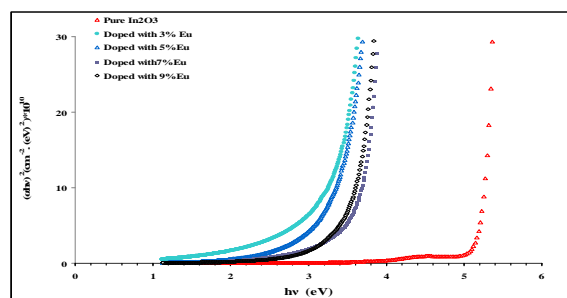


Fig. 7: Variation of $(\alpha hv)^2$ versus (hv) for the Eu-doped In_2O_3 thin films obtained at different doping ratio.

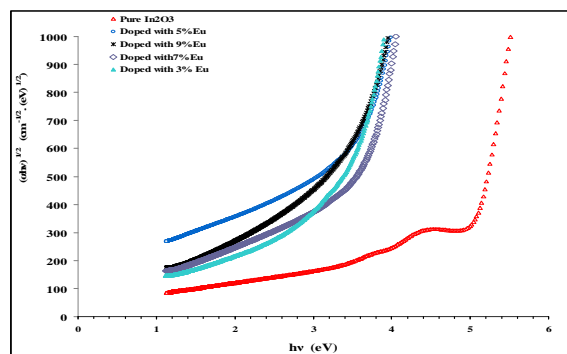


Fig. 8: Variation of $(\alpha hv)^{1/2}$ versus (hv) for the Eu-doped In_2O_3 thin films obtained at different doping ratio.

Table 2: The optical parameters of $\text{In}_2\text{O}_3:\text{Eu}$ thin films.

Sample	T%	α (cm^{-1})	k	n	ϵ_r	ϵ_i	E_g (eV)direct	E_g (eV)indirect
Pure In_2O_3	85.30	7951	0.032	2.086	4.352	4.352	5.20	4.9
Doped with 3%Eu	54.45	69908	0.284	2.995	8.889	8.889	3.18	3.2
Doped with 5%Eu	22.03	48018	0.191	9.019	81.307	81.307	3.20	3.26
Doped with 7%Eu	39.33	36963	0.147	5.819	33.837	33.837	3.50	3.40
Doped with 9%Eu	32.78	28338	0.113	7.628	58.166	58.166	3.50	3.30

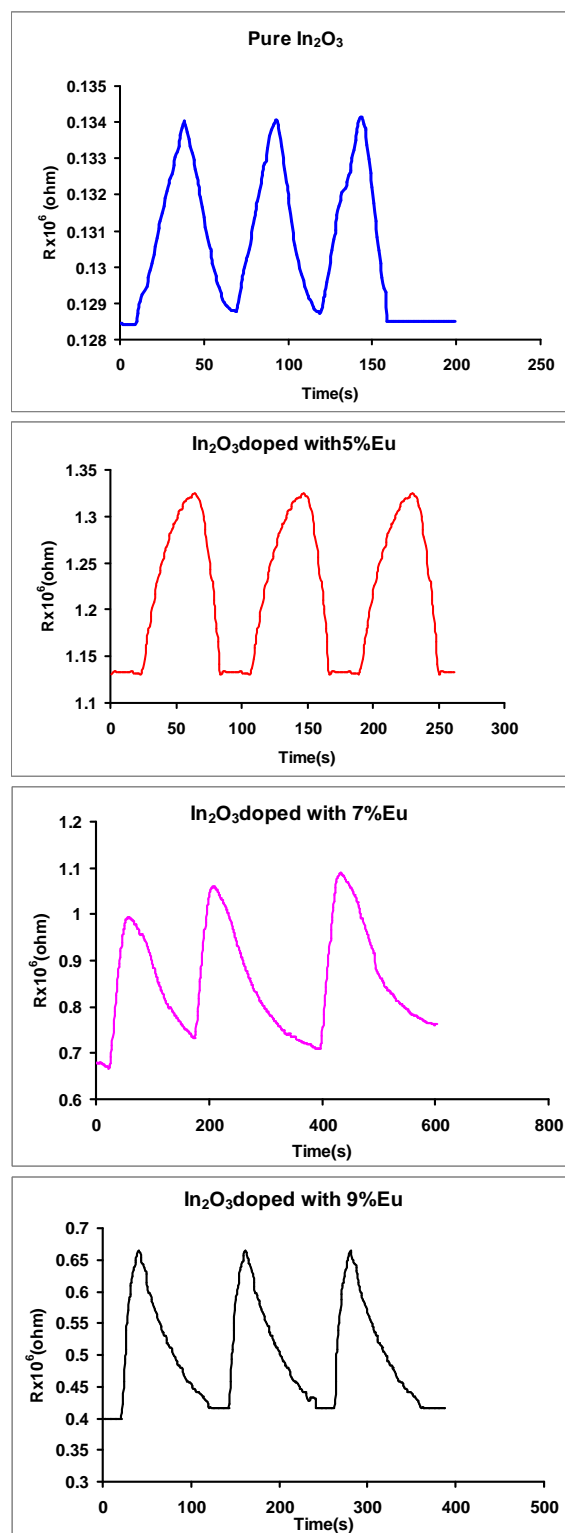


Fig. 9: The dynamic response versus recovery time cycle for for $\text{In}_2\text{O}_3:\text{Eu}$ thin films sensors.

Conclusions:

Thin films of undoped and Eu doped In_2O_3 with different doping ratio in the range (3,5,7, 5 and 9%) were prepared on glass and single crystal silicon substrates by spray pyrolysis method at room temperatures. Results shows that the doping is considered as main parameters which has significant effect of structural and sensing properties of the prepared films. Furthermore, structural, optical and electrical properties of the films were studied and optimized conditions are obtained. The X-ray diffraction patterns showed that the all undoped and doped thin films which were deposited with different doping ratio were polycrystalline. The gas sensing

analysis reveals that the gas sensitivity is higher for pure samples which contains both higher surface roughness and electrical resistivity.

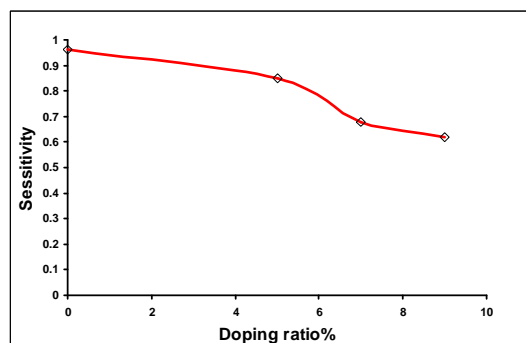


Fig. 10: Sensitivity versus doping ratio for $\text{In}_2\text{O}_3:\text{Eu}$ thin films sensors.

REFERENCES

- Fortunato, E., D. Ginley, H. Hosono, D.C. Paine, 2007. *Mater. Res. Soc. Bull.*, 32: 242.
- Hara, K., K. Sayama, H. Arakawa, 2000. *Solar Energy Mater. Solar Cells*, 62: 441.
- Biyikli, N., T. Kartoglu, O. Aytur, I. Kimukin, E. Ozbay, 2001. *Appl. Phys. Lett.*, 79: 2838.
- Vygranenko, Y., K. Wang, A. Nathan, 2007. *Appl. Phys. Lett.*, 91: 263508.
- Wang, L., M.H. Yoon, G. Lu, Y. Yang, A. Facchetti, T.J. Marks, 2006. *Nat. Mater.*, 5: 893.
- Dixit, A., C. Sudakar, R. Naik, V.M. Naik, G. Lawes, 2009. *Appl. Phys. Lett.*, 95: 192105
- Kaleemulla, S., A. Sivasankar Reddy, S. Uthanna, P. Sreedhara Reddy, 2007. *Mater. Lett.*, 61: 4309.
- Subrahmanyam, A., U.K. Barik, 2005. *J. Phys. Chem. Solids*, 66: 817.
- Radhakrishna, B., T.K. Subramanyam, B. Srinivasulu Naidu, S. Uthanna, 2000. *Opt. Mater.*, 15: 217.
- Subrahmanyam, A., U.K. Barik, 2006. *J. Phys. Chem. Solids*, 67: 1518.
- Chen, L.C., S.C. Liu, 2006. *Solid State Electron*, 50: 1355.
- Huang, M.H., Y. Wu, H. Feick, N. Tran, E. Weber, P. Yang, 2001. *Adv. Mater.*, 13: 113.
- Bourlang, A., D.J. Payne, R.G. Egdell, J.S. Foord, P.P. Edwards, M.O. Jones, A. Schertel, P.J. Dobson, J.L. Hutchison, 2008. *Appl. Phys. Lett.*, 92: 092117.
- Prathap, P., Y.P. Venkata Subbaiah, M. Devika, K.T. Ramakrishana Reddy, 2006. *J.Mater. Chem. Phys.*, 100-375.
- Sailer, R.A., A.Wanger, C. Schmit, N. Klaverkamp, D.L. Schulz, 2008. *Surf. Coat. Technol.*, 203-835.
- Flores, M.A., R. Castanedo, G. Torres, J. Marquez, O. Zelaya, 2008. *Thin Solid Films*, 570- 681.
- Moholkar, A.V., C.M. Pawar, K.Y. Rajpure, V. Ganesan, C.H. Bhosale, J. Alloys, 2008. *Compd.*, 464-387.
- Ghimbeu, C.M., J. Schoonman, M. Lumbieras, 2008. *Ceram. Int.*, 34-95.
- Klopffer, W., 1984. "Introduction to Polymer Spectroscopy", Springer – Verlag.
- Ho, W.H., C.F. Li, H.C. Liu, S.K. Yen, 2008. *J. Power Sources*, 175-897.
- Tauc, J., 1974. *Amorphous and Liquid Semiconductors*, Plenum Press.
- Pankov, J., 1971. *Optical Process in Semiconductors*, London.
- Korotcenkov, G., M. Nazarov, M.V. Zamoryanskaya, M. Ivanov, 2007. *Thin Solid Films*, 515: 8065.
- Rozati, S.M., T. Ganj, 2004. *Renew. Energy*, 29: 1665. [<http://dx.doi.org/10.1016/j.renene.2004.01.007>].
- Parthibab, S. V. Gokulakrishnan, K. Ramamurthi, E. Elangovan, R. Martins, E. Fortunato, R. Ganenan, 2009. *Solar Energy Mater. Solar Cells*, 93-92.
- Jeong S.H., S. Kho, D. Jung, S.B. Lee, J.H. Boo, 2003. Deposition of aluminum-doped zinc oxide films by RF magnetron sputtering and study of their surface characteristics, *Surface and Coatings Technology*, 174–175: 187–192.
- Greene, L.E., M. Law, J. Goldberger, F. Kim, J.C. Johnson, Y. Zhang, R.J. Saykally and P. Yang, 2003. *Angew. Chem. Int. Ed.*, 42: 3031 [<http://dx.doi.org/10.1002/anie.200351461>].
- Burstein, E., 1952. *Phys. Rev.*, 93: 632.
- Mott and Davis, 1979. *Electronic Process in Non Crystalline Semiconductors*, 2nd edition, University Press. Oxford.
- Korotcenkov, G., V. Brinzari, A. Cernevschi, M. Ivanov, V. Golovanov, A. Cornet, J. Morante, A. Cabot, J. Arbiol, 2004. *Thin Solid Films*, 460-315 [<http://dx.doi.org/10.1016/j.tsf.2004.02.01>].
- Korotcenkov, G., V. Brinzari, A. Cernevschi, M. Ivanov, A. Cornet, J. Morante, A. Cabot, J. Arbiol, 2004. *Sensors and Actuators B.*, 98-122 [<http://dx.doi.org/10.1016/j.snb.2003.09.009>].